Analysis of Traffic Flow With Mixed Manual and Semiautomated Vehicles

Arnab Bose, *Member, IEEE*, and Petros A. Ioannou, *Fellow, IEEE*

***Abstract*—The introduction of semiautomated vehicles designed to operate with manually driven vehicles is a realistic near-term objective. The purpose of this paper is to analyze the effects on traffic-flow characteristics and environment when semiautomated vehicles with automatic vehicle following capability (in the same lane) operate together with manually driven vehicles. We have shown that semiautomated vehicles do not contribute to the slinky effect phenomenon when the lead manual vehicle performs smooth acceleration maneuvers. We have demonstrated that semiautomated vehicles help smooth traffic flow by filtering the response of rapidly accelerating lead vehicles. The accurate speed tracking and the smooth response of the semiautomated vehicles designed for passenger comfort reduces fuel consumption and levels of pollutants of following vehicles. This reduction is significant when the lead manual vehicle performs rapid acceleration maneuvers. We have demonstrated using simulations that the fuel consumption and pollution levels present in manual traffic can be reduced during rapid acceleration transients by 28.5% and 1.5%–60.6%, respectively, due to the presence of 10% semiautomated vehicles. These environmental benefits are obtained without any adverse effects on the traffic-flow rates. Experiments with actual vehicles are used to validate the theoretical and simulation results**

***Index Terms*—Environmental savings, semiautomated vehicle, string stability, traffic flow.**

I. Introduction

RECENT advances in technology have propelled efforts to automate vehicles in order to achieve safe and efficient use of the current highway system. Fully automated vehicles that are able to operate autonomously in a highway environment are a long-term goal. On the other hand, partially or semiautomated vehicles designed to operate with current manually driven vehicles in today's highway traffic are seen as a more near-term objective. Their gradual penetration into the current highway system will usher the stage of mixed traffic where semiautomated vehicles will coexist with manually driven ones.

Considering the current penetration of products such as anti-lock braking systems (ABS), air bags, and cruise control into the vehicle market, it is justifiable to expect that intelligent cruise control (ICC) systems that give vehicles the capability to follow each other automatically in the same lane, will be deployed in the U.S. in the near future and penetrate the market in a similar fashion. Several major car manufacturers in Japan are already producing vehicles for sale with an ICC option. ICC is the next step to cruise control. It allows a vehicle to automatically follow another vehicle in a single lane using automatic throttle and brake controllers [1] in conjunction with various on-board sensors [15]. We refer to vehicles with ICC capability as semiautomated vehicles since they provide automation only in the longitudinal direction [2]. The driver is still responsible for lateral control of the semiautomated vehicle. In the initial stages, ICC may be designed as a driver-assist device and the driver will be responsible for crucial tasks like collision avoidance. Such a system may require the use of a fairly large intervehicle spacing (compared to the average used in today's driving) in an effort to account for possible larger driver reaction times due to the use of automation. As drivers become accustomed to the system and human factors and technical issues are resolved, ICC could be upgraded to have a longitudinal frontal collision avoidance (FCA) system [3]. In that case, the intervehicle spacing could be reduced considerably which could result into significant improvements in highway capacity.

Human factor considerations dictate that the response of an ICC vehicle should be smooth. As a result, an ICC vehicle is expected to act as a filter in vehicle following attenuating disturbances and smoothing traffic flow. Meanwhile, the vehicle–highway system is one of the major contributors to air pollution in urban areas due to increasing vehicle miles traveled and congestion [5]. With the gradual penetration of semiautomated vehicles into manual traffic, the question is whether the different dynamical response of semiautomated vehicles will have any impact on the environment and characteristics of traffic flow.

In this paper, we examine the effect of semiautomated vehicles on the transient behavior of traffic flow at the microscopic level when they operate together with manually driven vehicles. In our analysis, we consider a human driver car following model [8], [9] and a model of a semiautomated vehicle [1]. These models are used to analyze the transient behavior during vehicle following for three different cases. In case 1, all vehicles are manually driven; in case 2, all vehicles are semiautomated; and in case 3, manual and semiautomated vehicles are mixed.

We have shown that in manual driving, a car-following model, namely, Pipes model [8], [9] models slinky-type effects [6], a phenomenon observed in today's traffic. Thus, we use the Pipes model to simulate manual vehicle dynamics and examine

Manuscript received March 15, 1999; revised May 19, 2003. This work is supported by the California Department of Transportation through PATH of the University of California. The Associate Editor for this paper was I. Chabini.

A. Bose is with Real-Time Innovations, Inc., Sunnyvale, CA 94089 USA (e-mail: arnab@ rti.com).

P. A. Ioannou is with the Department of Electrical Engineering, University of Southern California, Los Angeles, CA 90089 USA (e-mail: ioannou@usc.edu).

Digital Object Identifier 10.1109/TITS.2003.821340

the effect of mixing manually driven and semiautomated vehicles on the traffic-flow characteristics during transients. Moreover, the response of the Pipes model is compared to actual manual vehicle responses involving different drivers. It is observed that slinky-type effects are more pronounced in actual manual driving than that modeled by the Pipes model. On the other hand, the semiautomated vehicle is modeled using an ICC design developed in [1] that is free of slinky-type effects and is designed to provide smooth driving at all times with the exception of emergencies.

Our analysis with mixed traffic shows that a "smooth" acceleration maneuver exhibited by a lead vehicle propagates upstream and gets amplified leading to the slinky effect phenomenon. In this case, the semiautomated vehicles do not contribute to the slinky effect since they are designed to respond to any smooth acceleration/velocity response in an accurate manner. When the lead vehicle exhibits a "rough" acceleration maneuver, the semiautomated vehicle in a mixed traffic situation acts as a filter by converting the "rough" acceleration response to a smooth response in an effort to maintain smooth driving. This is done at the expense of larger position, velocity, and acceleration errors and sometimes at the expense of falling far behind the vehicle ahead. We have shown that these characteristics of the semiautomated vehicles have a very beneficial effect on fuel economy and pollution that is significant during rapid acceleration transients. Simulations are used to quantify these benefits using the Pipes model [8], [9] and the ICC model developed in [1]. We demonstrate that the fuel consumption and pollution levels present in manual traffic can be reduced during smooth acceleration maneuvers by 8.5% and 8.1%–18.4%, respectively, and during rapid acceleration transients by 28.5% and 1.5%–60.6%, respectively, due to the presence of 10% semiautomated vehicles. It is demonstrated that these environmental benefits are obtained without any adverse effects on the traffic flow rate.

The quantitative benefits obtained using simulations were validated by experiments using three manually driven and semiautomated vehicles. The simulation results were repeated for the three vehicles modeled by the Pipes model and the ICC model using exactly the same driving scenarios as in the experiment. The comparison shows that the experiments validate the simulation results. Our analysis also indicates that the environmental benefits obtained in mixed traffic during vehicle transient responses are not at the expense of traffic-flow rates.

The paper is organized as follows. In Section II, we outline the concept of string stability in vehicle following and in Sections III and IV we analyze human driver car following and semiautomated vehicle models for string stability, respectively. We then extend our analysis into the case of mixed manual/semiautomated vehicles in Section V. In Section VI, we perform simulations for different car following scenarios in manual and mixed traffic and confirm the analytical findings. In this section we also compare the responses of the Pipes model with that of an actual manually driven vehicle. In Section VII, we discuss the environmental results using simulations and experiments with actual vehicles. In Section VIII, we examine the effect of traffic disturbances due to rapid vehicle acceleration transients on mixed traffic flow. We present our conclusions in Section IX

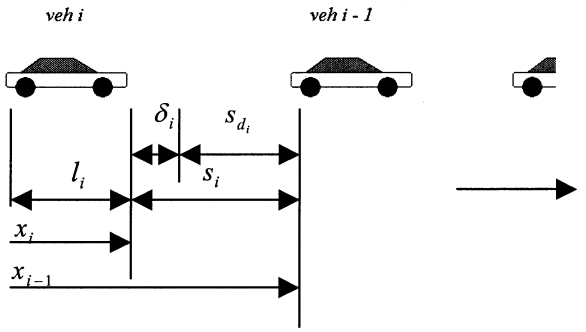

Fig. 1. Interconnected system of vehicles following each other in a single lane.

II. Two String Stability: Mathematical Definitions

In vehicle following, the dynamics of each vehicle are coupled with other vehicles leading to a larger dynamical system. Even though each vehicle may have stable behavior and good performance, the behavior of the overall coupled system may not be desirable. For example, transients caused by a single vehicle changing its speed may be amplified upstream leading to what is known as "slinky-type effect" [6] or string instability. String stability [17] in vehicle following implies that any nonzero position, velocity, and acceleration error of an individual vehicle in a string of vehicles do not get amplified as it propagates upstream. We begin by giving the mathematical definitions of string stability for interconnected systems of vehicles closely following each other in a single lane. Next, microscopic human driver car following and semiautomated vehicle models are used to investigate string stability in manual, semiautomated vehicular, and mixed traffic situations. Finally, we perform a series of simulations to illustrate different manual and mixed-traffic vehicle following scenarios.

A system of vehicles in a single lane under moderately dense traffic conditions can be considered as a countable infinite interconnected system. For simplicity, i.e., to avoid boundary conditions, we consider the system to consist of infinite subsystems. If a system comprises of finite number of subsystems, it can be treated as if the number were infinite by assuming fictitious subsystems at both ends. Such a system shown in Fig. 1 can be modeled as [18]

$$v_i = G_i(s)v_{i-1} \tag{1}$$

where $i \in N$, and N is the number of vehicles considered, v_i is the longitudinal speed of the ith vehicle, and $G_i(s)$ is a proper stable transfer function that represents the input–output dynamics of the ith vehicle in the longitudinal direction. The system represents traffic in a single lane without passing in which every vehicle tries to match the speed of the preceding vehicle with some precision and vehicle spacing. The details of the dynamics of such a system are often described by complex nonlinear dynamical models. Such models are linearized about an operating speed to put them in the framework of (1), without affecting the accuracy of the response within the operating range of interest.

Definition 1 (Class of Interconnected Systems): The class of interconnected systems consists of interconnected systems that satisfy (1).

Let us define the following errors for the ith vehicle as

$$\begin{aligned}\delta_i &= s_i - s_{d_i} = x_{i-1} - x_i - l_i - s_{d_i} \quad \text{(position error)}\\ v_{ri} &= v_{i-1} - v_i \quad \text{(velocity error)}\\ a_{ri} &= a_{i-1} - a_i \quad \text{(acceleration error)}\end{aligned}$$

where

- x_i abscissa of the rear bumper of the ith vehicle
- s_{d_i} desired intervehicle spacing followed by the ith vehicle
- s_i actual intervehicle spacing measured from the rear of the $i-1$ vehicle to the front of the ith vehicle
- l_i length of the ith vehicle
- δ_i deviation between the actual and the desired intervehicle spacing, also referred to as the position error
- v_i velocity of the ith vehicle
- a_i acceleration of the ith vehicle.

Definition 2 (String Stability): The interconnected system of vehicles given in (1) is *string stable* if the position, velocity and acceleration errors do not amplify when they propagate upstream, i.e.,

$$\begin{aligned}&\|\delta_i\|_p \le \|\delta_{i-1}\|_p\\ &\|v_{ri}\|_p \le \|v_{ri-1}\|_p \quad \forall\, p \in [1,\infty],\ \forall\, i \in N\\ &\|a_{ri}\|_p \le \|a_{ri-1}\|.\end{aligned} \tag{2}$$

Definition 3 (Strict String Stability): The interconnected system of vehicles given in (1) is *strictly string stable* if the position, velocity and acceleration errors attenuate when they propagate upstream, i.e.,

$$\begin{aligned}&\|\delta_i\|_p < \|\delta_{i-1}\|_p\\ &\|v_{ri}\|_p < \|v_{ri-1}\|_p \quad \forall\, p \in [1,\infty],\ \forall\, i \in N\\ &\|a_{ri}\|_p < \|a_{ri} - 1\|_p.\end{aligned} \tag{3}$$

Definition 4 (String Unstable): The interconnected system of vehicles given in (1) is said to be *string unstable* if it does not satisfy (2) for any $i \in N$ or for any $p \in [1,\infty]$.

1) Case 1: Vehicles With Constant Vehicle Spacing: Let us consider the case where the desired intervehicle spacing s_{d_i} is constant at all speeds. Consider a string of vehicles with different transfer functions $G_i(s)$ that satisfy (1). We have

$$\begin{aligned}\delta_i &= x_{i-1} - x_i - l_i - s_{d_i}\\ \delta_i &= \frac{1}{s}[v_{i-1} - v_i] - l_i - s_{d_i}\end{aligned}$$

where "s" is the Laplace operator.

For string stability analysis we focus on the upstream propagation of transient position/velocity/acceleration errors. During such transients, we have $sl_i = ss_{d_i} = 0$ for constant vehicle length l_i and constant intervehicle spacing s_{d_i}. Thus, neglecting these noncontributing terms, since they have no effect on the transient position error analysis, we have

$$\begin{aligned}\delta_i &= \frac{1}{s}(1 - G_i)v_{i-1}\\ v_{ri} &= v_{i-1} - v_i = (1 - G_i)v_{i-1}\\ a_{ri} &= \dot{v}_{ri} = \dot{v}_{i-1} - \dot{v}_i\end{aligned}$$

or

$$a_{ri} = s(1 - G_i)v_{i-1}$$

which shows that

$$\frac{\delta_i}{\delta_{i-1}} = \frac{v_{ri}}{v_{ri-1}} = \frac{a_{ri}}{a_{ri-1}} = \frac{(1 - G_i)}{(1 - G_{i-1})}G_{i-1} = \bar{G}_i(s). \tag{4}$$

Remark 1: When all the vehicles have identical input–output characteristics, i.e., $G_i(s) = G(s)$, then $\bar{G}_i(s) = G(s)$.

Instead of the constant intervehicle spacing policy, we may have vehicles with constant time headway policy, in which case the desired intervehicle spacing is proportional to the vehicle speed and the proportionality constant is known as the time headway. Time headway is defined as the time it takes for a vehicle to cover the distance measured from the rear of the front vehicle to the front of the following vehicle. It can be shown that when all the vehicles in the fleet have identical input–output characteristics, i.e., $G_i(s) = G(s)$, then (4) holds also for the constant time headway policy with $\bar{G}_i(s) = G(s)$. However, the case when they have different input–output characteristics warrants further investigation.

2) Case 2: Vehicles With Constant Time Headway Policy: Let us consider the case where the vehicles use a constant time headway policy, i.e., the desired intervehicle spacing s_{d_i} is equal to the constant time headway multiplied by the vehicle speed. Let us now consider a string of vehicles that satisfy (1). The position error is given by

$$\delta_i = x_{i-1} - x_i - l_i - h_i\dot{x}_i$$

where h_i is the time headway of the ith vehicle. Using the Laplace operator "s," we have

$$\delta_i = \frac{1}{s}[v_{i-1} - v_i] - l_i - h_i\dot{x}_i.$$

For string stability analysis we focus on the upstream propagation of transient position/velocity/acceleration errors. During such transients we have $sl_i = 0$ for constant vehicle length l_i. Thus, neglecting this noncontributing term, since it does not affect the transient position error analysis, we have

$$\begin{aligned}\delta_i &= \frac{1}{s}[v_{i-1} - v_i] - h_i v_i = \frac{1}{s}[1 - G_i - sh_iG_i]v_{i-1}\\ v_{ri} &= v_{i-1} - v_i = (1 - G_i)v_{i-1}\\ a_{ri} &= \dot{v}_{ri} = \dot{v}_{i-1} - \dot{v}_i\end{aligned}$$

or

$$a_{ri} = s(1 - G_i)v_{i-1}$$

which gives us

$$\frac{\delta_i}{\delta_{i-1}} = \frac{1 - G_i - sh_iG_i}{1 - G_{i-1} - sh_{i-1}G_{i-1}}G_{i-1} = \hat{G}_i(s) \tag{5}$$

and

$$\frac{v_{ri}}{v_{ri-1}} = \frac{a_{ri}}{a_{ri-1}} = \frac{(1 - G_i)}{(1 - G_{i-1})}G_{i-1} = \bar{G_i}(s).$$

Theorem 1 (String Stability): The class of interconnected systems of vehicles following each other in a single lane without passing is *string stable* if and only if the impulse response $g_i(t)$ of the error propagation transfer function $G_i(s)$, $\bar{G}_i(s)$, or $\hat{G}_i(s)$, as the case may be, for each individual vehicle in this class satisfies

$$\|g_i\|_1 \le 1 \quad \forall\ i \in N. \tag{6}$$

Proof:

If: Assuming $\delta_i, v_{ri}, a_{ri} \in L_p$ and $g_i \in L_1$ where $i \in N$, we have from [7]

$$\begin{aligned} ||\delta_i||_p &\le ||g_i||_1 ||\delta_{i-1}||_p \\ ||v_{ri}||_p &\le ||g_i||_1 ||v_{ri-1}||_p \quad \forall\, p \in [1, \infty] \\ ||a_{ri}||_p &\le ||g_i||_1 ||a_{ri-1}||_p. \end{aligned} \tag{7}$$

Therefore, if we have $||g_i||_1 \le 1\ \forall\, i \in N$, then (2) of Definition 2 is satisfied and the system is string stable.

Only If: It can be shown that if condition (6) is not met, then there exists a position error signal that will lead to string instability for a particular transfer function that does not belong to the *class* of interconnected systems defined in the theorem. For example, if

$$G_i(s) = \frac{s+2}{s^2+s+1}$$

we have

$$g_i(t) = e^{-0.5t}\cos(0.87t) + 1.732e^{-0.5t}\sin(0.87t)$$

and

$$||g_i||_1 > 1$$

Consider the error signal

$$\delta_{i-1}(t) = \begin{cases} 1, & 0 \le t \le t' \\ 0, & \text{otherwise} \end{cases}$$

such that $||\delta_{i-1}||_\infty = 1$ and $\delta_{i-1} \in L_p$. We have

$$\begin{aligned} \delta_i(t) &= \int_0^t g_i(t-\tau)\delta_{i-1}(\tau)d\tau = -1.993e^{-0.5t}\cos(0.87t) \\ &\quad + .004e^{-0.5t}\sin(0.87t) + 1.993, \quad t < t' \\ &= \int_0^{t'} g_i(t-\tau)\delta_{i-1}(\tau)d\tau = -1.993e^{-0.5t}\cos(0.87t) \\ &\quad + 0.004e^{-0.5t}\sin(0.87t) \\ &\quad + 1.993e^{-0.5(t-t')}\cos(0.87(t-t')) \\ &\quad - 0.004e^{-0.5(t-t')}\sin(0.87(t-t')), \qquad t \ge t'. \end{aligned}$$

Say $t' = 10$, then we get $||\delta_i||_\infty \approx 2.4 > ||\delta_{i-1}||_\infty$ which implies string instability by Definition 4. Similarly, it can be also shown that $||v_{ri}||_\infty > ||v_{ri-1}||_\infty$ and $||a_{ri}||_\infty > ||a_{ri-1}||_\infty$ for similar velocity and acceleration error signals. ■

Remark 2:

i) We should note that the string stability theorem refers to a *class* of systems. For example, the *class* of systems characterized by $||g_i||_1 \le 1\ \forall\, i \in N$ is string stable. The *class* of systems with $||g_i||_1 > 1$ for some i cannot be guaranteed to be string stable because we can find at least one system in this class that is string unstable. This, however, does not mean that every system with $||g_i||_1 > 1$ for some i is string unstable. This is due to the fact that the condition $||g_i||_1 \le 1$ is obtained from an inequality that could be conservative.

ii) In addition to string stability, it is desirable to have $g_i(t) > 0\ \forall\, i \in N\ \forall\, t > 0$ in order to avoid oscillatory responses [6].

Lemma 1 (Strict String Stability): The *class* of interconnected systems of vehicles following each other in a single lane without passing is *strictly string stable* if and only if the impulse response $g_i(t)$ of the error propagation transfer function $G_i(s)$, $\bar{G}_i(s)$, or $\hat{G}_i(s)$, as the case may be, for each individual vehicle in this class satisfies

$$||g_i||_1 < 1 \quad \forall\, i \in N. \tag{8}$$

Proof: It is similar to the earlier proof and is omitted. ■

Remark 3: For the interconnected system of vehicles that we consider in (1), the ICC controllers of the vehicles are designed such that at steady state (zero frequency), the velocity of the following vehicle matches that of the preceding vehicle. This means that we will always have $|G_i(0)| = 1\ \forall\, i \in N$.

It is also desirable to design $G_i(s)$ so that $g_i(t)$ does not change sign in order to avoid oscillatory responses in the error signals that could give rise to undesirable speed fluctuations in traffic flow. If the ICC controllers are designed to guarantee that $g_i(t)$ does not change sign and $|G_i(0)| = 1$, then string stability is guaranteed as stated by the following lemma.

Lemma 2: Assume that $G_i(s)$ is designed so that $g_i(t)$ does not change sign and $|G_i(0)| = 1$. Then the system of N vehicles with transfer function $G_i(s)$, $i \in N$ is string stable.

Proof: If the impulse response $g_i(t)$ does not change sign we have

$$||g_i||_1 = \int_0^\infty |g_i(t)|dt = |\int_0^\infty g_i(t)e^{-0t}dt| = |G_i(0)| = 1. \tag{9}$$

Therefore, condition (2) of Definition 2 is satisfied and the string of vehicles is string stable. ■

Remark 4: A less conservative bound could be obtained in (7) when $p = 2$. In this case, we have [7]

$$\begin{aligned} ||\delta_i||_2 &\le ||G_i(s)||_\infty ||\delta_{i-1}||_2 \\ ||v_{ri}||_2 &\le ||G_i(s)||_\infty ||v_{ri-1}||_2 \\ ||a_{ri}||_2 &\le ||G_i(s)||_\infty ||a_{ri} - 1||_2 \end{aligned} \tag{10}$$

where

$$||G(s)||_\infty = \sup_\omega |G(j\omega)|$$

and from [7]

$$||G_i(s)||_\infty \le ||g_i||_1. \tag{11}$$

Remark 5: Since $v_i = G_i(s)v_{i-1}$, it follows that for speed following matching at steady state we should have $|G_i(0)| = 1$ which means that $||G_i(s)||_\infty \ge 1$. This, in turn, means that the best we can do in (10) is to design $G_i(s)$ so that $||G_i(s)||_\infty = 1$. Another approach is to design $G_i(s)$ so that $|G_i(0)| = 1$ and $|G_i(j\omega)| < 1\ \forall\, \omega > 0$. In this case, we will have strict string stability ($||\delta_i||_2 < ||\delta_{i-1}||_2$, $||v_{ri}||_2 < ||v_{ri-1}||_2$, $||a_{ri}||_2 < ||a_{ri-1}||_2$) for frequencies $|\omega| > 0$. This approach has already been used in [1], [6].

Remark 6: It should be noted that our definition for string stability is conservative. In other words, if (2) is violated for some i, that does not mean that the response of the string of vehicles is not acceptable. The mixing of vehicles with $G_i(s)$ that satisfies for some i and violates for some other i the conditions of the string stability theorem (6) will be analyzed in Section V.

III. String Stability of Manual Traffic

We investigate the string stability of a fleet of manual vehicles closely following each other in a single lane using a human driver car following model from the literature. The model is applicable only under conditions of fairly dense traffic in which the driver generally attempts to match his velocity to the car ahead while maintaining some intervehicle spacing. The string stability theorem is used to examine whether the model belongs to the class of systems that guarantee string stability. We assume that all vehicles in the fleet have identical input–output characteristics and so by Remark 1 we have the following:

$$\frac{\delta_i}{\delta_{i-1}} = \frac{v_{ri}}{v_{ri-1}} = \frac{a_{ri}}{a_{ri-1}} = \frac{v_i}{v_{i-1}} = G_i(s) = G(s).$$

Thus, to investigate whether the following models belong to the class of systems that guarantee string stability, we analyze the transfer function of each model that relates the velocity of the lead vehicle to that of the following vehicle.

A. Pipes Model

This is a linear follow-the-leader model based on car following theory that pertains to single-lane dense traffic with no passing and assumes that each driver reacts to a stimulus from the vehicle ahead. The stimulus is the velocity difference and the driver responds with an acceleration command, i.e.,

$$\text{Response}(t) = \text{Sensitivity} \times \text{Stimulus}(t - \tau)$$

where τ is the reaction time of the driver–vehicle system.

It can be mathematically expressed as

$$a_f = \frac{\lambda}{M}[v_l(t-\tau) - v_f(t-\tau)] \tag{12}$$

where v_l and v_f are the lead and following vehicles' velocities, respectively, a_f is the following vehicle's acceleration, M is the mass of the following vehicle, and λ is a sensitivity factor. The dynamics of the vehicle are modeled by an integrator and the driver's central processing and neuromuscular dynamics by a constant. This model was first proposed by Pipes [8] and later validated by Chandler [9].

The transfer function of the Pipes model is given by

$$G_p(s) = \frac{v_i}{v_{i-1}} = \frac{0.37e^{-1.5s}}{s + 0.37e^{-1.5s}}. \tag{13}$$

Evaluating the impulse response we get $||g_p||_1 = 1.1$, implying that the Pipes model does not belong to the class of systems mentioned in the theorem [given by (6)] that guarantee string stability. However, we cannot confirm the existence of slinky effect. Also, $g_p(t)$ changes sign for $t > 0$ (Fig. 2), which means that the model has an oscillatory response. We also find that for very small frequencies. As we demonstrate later using simulations, a string of vehicles represented by the Pipes model exhibits string instability. Furthermore, a comparison of the responses of the Pipes model with experiments presented in Section VI shows that the Pipes model gives a response that is less oscillatory with smaller slinky-type effects than in actual vehicles. Consequently, in actual driving one would expect more pronounced slinky-type effects than those predicted by the Pipes model. One reason for this discrepancy is that the human driver models were developed and validated for relatively smooth vehicle following. Among the several human driving models considered the response of the Pipes model was found to be the closest to the one observed during experiments in the presence of transients.

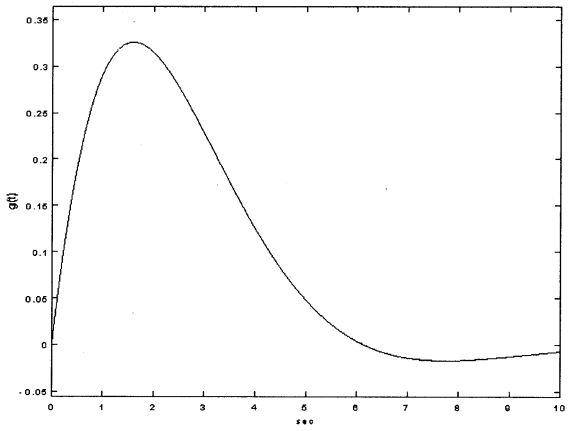

(a)

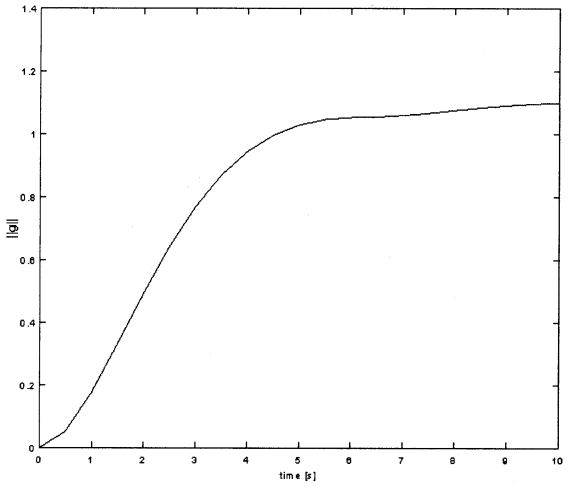

(b)

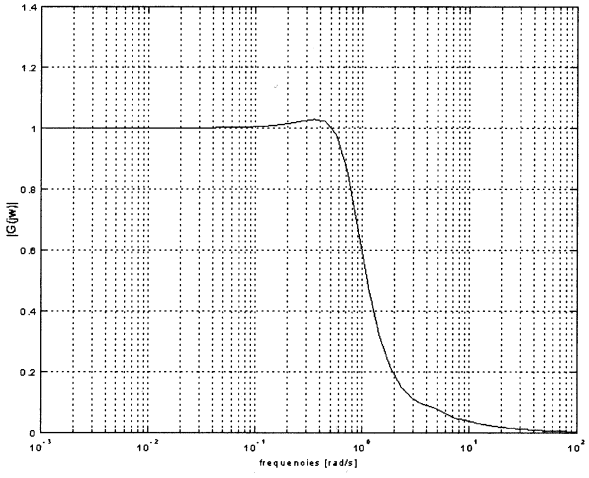

(c)

Fig. 2. Pipes linear car following model. (a) Impulse response $g_p(t)$ versus t. (b) $\int_0^t |g_p(\tau)|d\tau$ versus t. (c) $|G_p(j\omega)|$ verus ω.

IV. String Stability of Semiautomated Traffic

Let us now consider the string stability of a fleet of semiautomated vehicles closely following each other in a single lane. The ICC model given in [1] is used to represent the semiautomated vehicles. For longitudinal control, the automatic control system of the semiautomated vehicle may be considered as having two input variables: throttle angle command and brake command, and one output variable: vehicle speed [1]. The other inputs such as aerodynamic drag, road conditions, and vehicle mass changes are treated as disturbances. The semiautomated vehicle is assumed to use a constant time headway policy. We consider the throttle and the brake subsystems separately, as they are not allowed to act simultaneously.

A. Throttle Controller

The closed-loop transfer function for the throttle subsystem is given by (14) [1] (at the bottom of the page), where

k_1, k_2, k_3, k_4 designed controller parameters;
h time headway desired;
a, b coefficients determined by the operating point which is the speed of the vehicle ahead.

The throttle controller is designed to control the throttle angle of the semiautomated vehicle using the design controller parameters k_1 to k_4 that are chosen using pole placement as follows [1]:

$$k_1 = \frac{(\lambda_0 + 2\zeta\omega_n - bk_2h - a)}{b}$$
$$k_2 = \frac{0.2}{b}$$
$$k_3 = \frac{(2\zeta\omega_n\lambda_0 + \omega_n^2 - bk_2 - h\lambda_0\omega_n^2)}{b}$$
$$k_4 = \frac{\lambda_0\omega_n^2}{b} \tag{15}$$

where

λ_0 desired pole;
ω_n, ζ natural frequency and damping ratio of the two desired complex poles, respectively.

The throttle controller in (14) is applied to a validated nonlinear vehicle model and tested through a series of simulations with the following parameter values that satisfy the performance criteria [1]:

$\lambda_0 = 1.2$, $\omega_n = 0.1$, $\zeta = 1$ and a constant time headway $h = 1s$.

Using these values in (15) to get the controller parameter values and substituting them in (14) we obtain

$$G_{th}(s) = \frac{1.2s^2 + 0.24s + 0.012}{s^3 + 1.4s^2 + 0.25s + 0.012}. \tag{16}$$

The L_1 norm of the throttle subsystem (16) is $\|g_{th}\|_1 = 1$. Also the impulse response $g_{th}(t) > 0$ for all $t > 0$ (Fig. 3). Thus, the throttle controller of the semiautomated vehicle

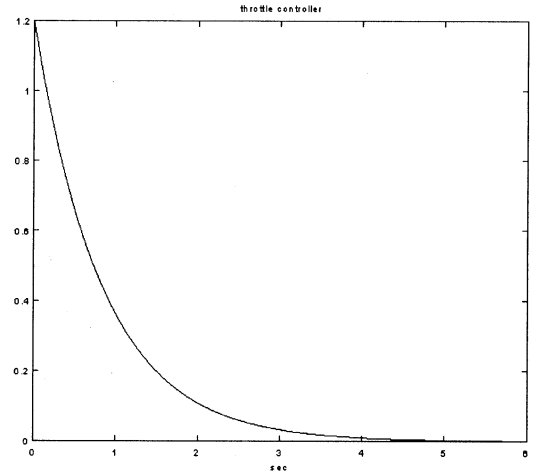

(a)

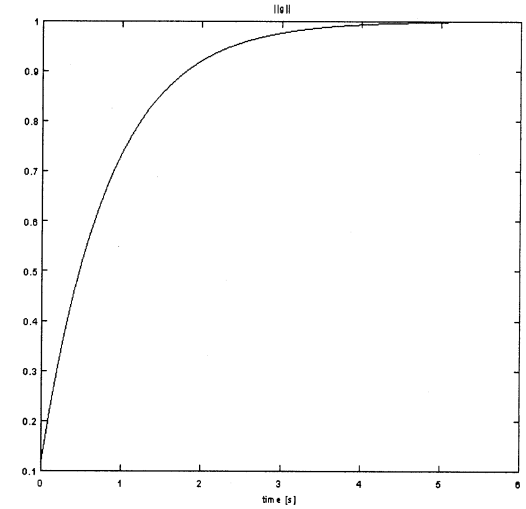

(b)

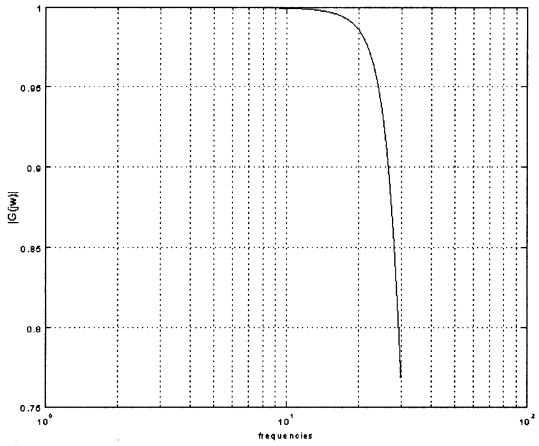

(c)

Fig. 3. Throttle controller subsystem. (a) Impulse response $g_{th}(t)$ versus t. (b) $\int_0^t |g_{th}(\tau)|d\tau$ versus t. (c) $|G_{th}(j\omega)|$ versus ω.

$$G_{th}(s) = \frac{\delta_i}{\delta_{i-1}} = \frac{(a + bk_1)s^2 + b(k_2 + k_3)s + bk_4}{s^3 + (a + bk_1 + bk_2h)s^2 + b(k_2 + k_3 + k_4h)s + bk_4} \tag{14}$$

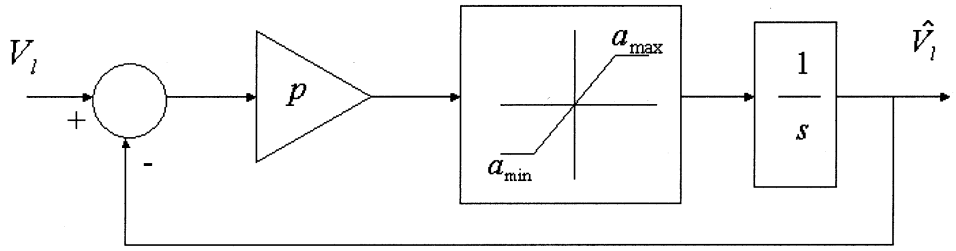

Fig. 4. Acceleration limiter.

belongs to the class of systems that guarantee string stability. Moreover, $|G_{th}(j\omega)|$ is less than unity for all $\omega > 0$.

Human factor considerations dictate that the response of a semiautomated vehicle should be smooth. Therefore, there are two constraints imposed on the throttle controller due to smooth ride requirements [1]. The constraints are the following.

C-I: $a_{\min} \leq \ddot{V}_f \leq a_{\max}$ where $a_{\min}$ and $a_{\max}$ are specified.

C-II: The absolute value of the jerk defined as $\dddot{V}_f$ should be as small as possible.

The controller in (16) does not guarantee that the above two constraints will always be satisfied. For example, if the lead vehicle rapidly changes its velocity at a particular point, it may create a large relative velocity error and spacing error, which in turn may cause large throttle angle and acceleration, violating C-I and C-II. Also, there may be large initial position and velocity errors when the following vehicle switches from one leading vehicle to another due to lane change, merging, etc., leading to high acceleration/deceleration that may violate C-I and C-II. In order to avoid these occurrences, two limiters are used in the throttle controller of [1].

The first is an acceleration limiter to protect the semiautomated vehicle from responding to erratic behavior of the leading vehicle. The velocity of the leading vehicle V_l is passed through an acceleration limiter shown in Fig. 4 where p is some positive constant. Instead of following V_l, the throttle controller is designed to follow $\hat{V}_l$. The acceleration limiter limits the maximum and minimum acceleration of the target velocity to $a_{\max}$ and $a_{\min}$, respectively. It eliminates any sudden changes in V_l during transients and presents a smooth target velocity for the controller to follow. At steady state, $\hat{V}_l$ approaches V_l, therefore, following the former the throttle controller will eventually reach V_l in a smooth way.

In 100% semiautomated traffic, the acceleration limiter will not affect string stability since all vehicles (with the exception of emergency stopping) are assumed to operate within the limits of $a_{\max}$ and $a_{\min}$. In mixed traffic this may not be the case because the manually driven vehicles may generate trajectories outside the desired acceleration limits.

In addition to the acceleration limiter, the spacing error is passed through a saturation element to take care of large spacing errors being fed into the controller. The saturation element $\mathrm{sat}(\delta)$ is defined as

$$\mathrm{sat}(\delta) = \begin{cases} e_{\max}, & \text{if } \delta > e_{\max} \\ e_{\min}, & \text{if } \delta < e_{\min} \\ \delta, & \text{otherwise.} \end{cases}$$

This prevents any large spacing error and limits the spacing error measurements seen by the throttle controller to be within $e_{\max}$ and $e_{\min}$. In other ICC designs, similar modifications are used to maintain smooth response.

B. Brake Controller

For the closed-loop brake subsystem we have the following transfer function [1]:

$$G_{br}(s) = \frac{v_i}{v_{i-1}} = \frac{k_5 s + k_6}{s^2 + (k_5 + k_6 h)s + k_6} \tag{17}$$

where

k_5, k_6 brake controller gains;

h time headway desired.

Equation (17) is investigated for $h = 1s$ with the following gains that satisfy the performance criteria given in [1]:

$$k_5 = 1 \quad k_6 = 0.25.$$

From the impulse response of (17) we have $\|g_{br}\|_1 = 1$ and $g_{br}(t) > 0$ for all $t > 0$ (Fig. 5), implying that the brake controller does not have an oscillatory response. Hence, like the throttle controller, the brake controller also belongs to the class of systems that guarantee string stability. Furthermore, $|G_{br}(j\omega)|$ is less than unity for all $\omega > 0$.

Therefore, we have shown that both the throttle and the brake subsystems belong to the class of systems that guarantee string stability provided that they remain within the saturation limits used. It is important to note that the design parameters of the controllers can be modified such that the throttle and the brake controller subsystems violate (6) and not belong to the class of systems that guarantee string stability.

V. String Stability of Mixed Vehicles

The mixed traffic system consists of manual and semiautomated vehicles whose dynamics are given by the models presented in Sections II–IV. Consider the manual vehicles to be represented by the Pipes model, which does not belong to the class of systems that guarantee string stability and may generate slinky-type effects. Therefore, we cannot guarantee string stability for the system of mixed vehicles.

However, as stated before, Definition 2 of string stability is conservative. Though the string of mixed vehicles may not be string stable, the behavior of the whole system may be acceptable. We carry out an analysis that should provide some insight into the dynamics of mixed traffic during transients. Consider vehicle following transients for two different cases.

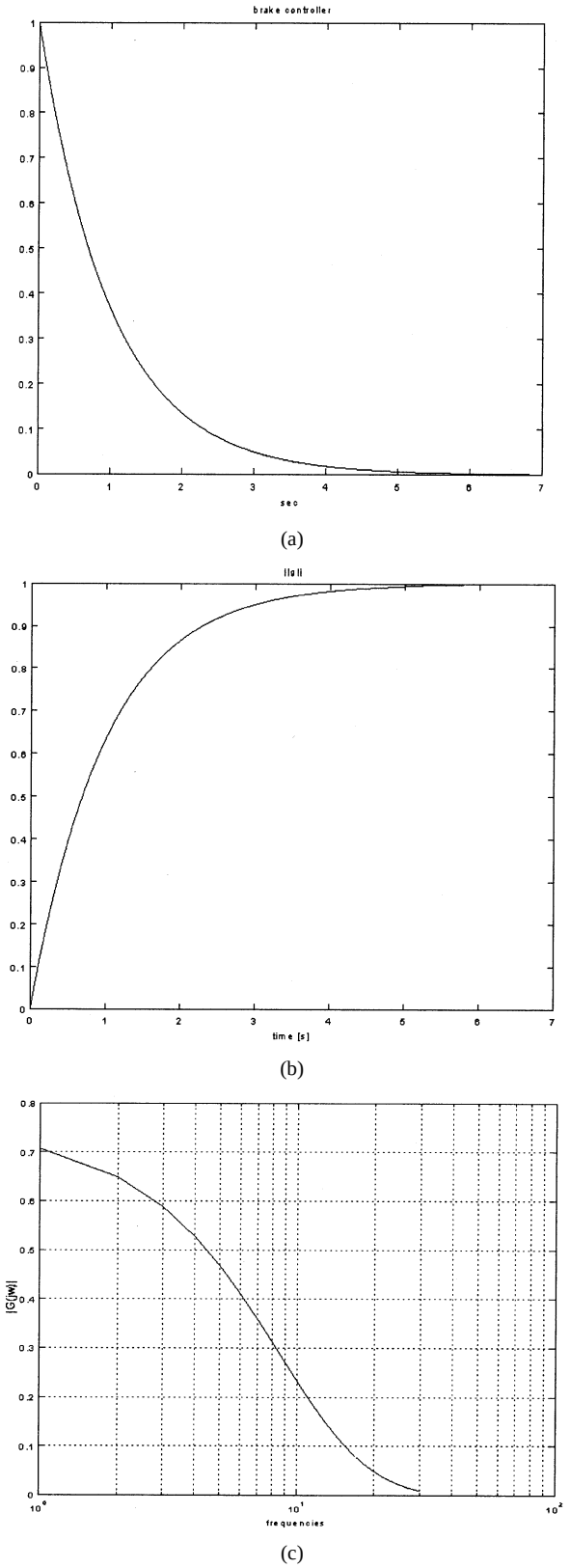

Fig. 5. Brake controller subsystem. (a) Impulse response $g_{br}(t)$ versus t. (b) $\int_0^t |g_{br}(\tau)|d\tau$ versus t. (c) $|G_{br}(j\omega)|$ versus ω.

A. Lead manual vehicle in mixed traffic performs a smooth acceleration maneuver.

B. Lead manual vehicle in mixed traffic performs a rapid acceleration maneuver.

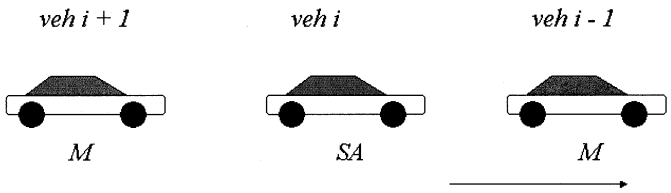

Fig. 6. Mixed manual/semiautomated traffic.

A. Lead Manual Vehicle in Mixed Traffic Performs a Smooth Acceleration Maneuver

Using the ICC model presented in Section IV to represent semiautomated vehicles, a smooth acceleration maneuver by a lead manual vehicle means that the target speed is within the saturation limits of the ICC acceleration limiter. Considering mixing of vehicles of different classes, we get the error propagation transfer functions as [from (4) and (5)]

$$\frac{\delta_i}{\delta_{i-1}} = \frac{1 - G_i - sh_iG_i}{1 - G_{i-1} - sh_{i-1}G_{i-1}} G_{i-1} = G_{ii-1}(s) \qquad (18)$$

$$\frac{v_{ri}}{v_{ri-1}} = \frac{a_{ri}}{a_{ri-1}} = \frac{(1 - G_i)}{(1 - G_{i-1})} G_{i-1} = \bar{G}_i(s). \qquad (19)$$

Examining (18), we can conclude that given $G_i(s)$ there may exist an $h_i \ni 1 - G_i(s) - sh_iG_i(s) = 0 \,\forall\, s$. The existence of such h_i is given by the following lemma.

Lemma 3: A constant h_i exists for a given $G_i(s) = n(s)/d(s)$ such that $1 - G_i(s) - sh_iG_i(s) = 0 \,\forall\, s$ if and only if degree $(d(s))$-degree $(n(s)) = 1$ and for

$$d(s) = s^n + a_1 s^{n-1} + \cdots + a_{n-1}s + a_n$$

and

$$n(s) = b_1 s^{n-1} + b_2 s^{n-2} + \cdots + b_{n-1}s + b_n$$

where $a_1, a_2, \ldots, a_n$, $b_1, b_2, \ldots, b_n$, are constants with $a_n = b_n$, the following is true:

$$\frac{b_{n-1}}{a_{n-1}b_1 - b_n} = \cdots = \frac{b_1}{a_1 b_1 - b_2} = \frac{1}{b_1} = h > 0 \qquad (20)$$

where $h_i = h$. The proof is simple and is omitted. ■

The existence of h_i to satisfy Lemma 3 exactly is a singular case. The use of h_i, however, guarantees that the following vehicle will maintain zero position, velocity and acceleration errors during vehicle following. In other words, with h_i the two vehicles, lead and following will be electronically connected and behave as a single vehicle. Choosing h_i to satisfy Lemma 3 is not practical. However, choosing a time headway close to h_i is possible leading to tight vehicle following. This is demonstrated in the following example.

Consider a string of mixed manual/semiautomated vehicles as depicted in Fig. 6. Vehicle i (SA) is a semiautomated vehicle while vehicle $i - 1(M)$ and the rest are manual vehicles. All vehicles are assumed to follow a constant time headway policy.

We choose Pipes model [8], [9] to represent manually driven vehicles since we demonstrate that it models the slinky-type effects we observe in today's traffic (Section VI). We assume that the semiautomated vehicles follow a time headway of $1.0s$. For manual vehicles, it is difficult to assume a fixed number since different drivers have different driving characteristics. However, for our analysis we assume that the manual vehicles follow a

time headway of $1.8s$, which is taken as the "national average" for manual traffic [16]. Therefore, we have

$$\frac{\delta_i}{\delta_{i-1}} = \frac{1 - G_{th} - sG_{th}}{1 - G_p - 1.8sG_p} G_p = G_{ii-1}(s) \qquad (21)$$

where $G_p(s)$ is taken from (13) and $G_{th}(s)$ is the transfer function of the throttle controller of the ICC vehicle. The time delay is approximated using

$$e^{-Ts} \approx \frac{1}{1+Ts}$$

to obtain

$$G_p(s) = \frac{0.37}{1.5s^2 + s + 0.37}$$

and from (16)

$$G_{th}(s) = \frac{1.2s^2 + 0.24s + 0.012}{s^3 + 1.4s^2 + 0.25s + 0.012}.$$

So after substituting for $G_p(s)$ and $G_{th}(s)$ in (21) and rearranging the terms, we have

$$\frac{\delta_i}{\delta_{i-1}} = -\frac{0.074s^3 + 0.014s^2 + 0.0007s}{1.5s^5 + 2.434s^4 + 0.8426s^3 + 0.1015s^2 + 0.004s} = G_{ii-1}(s).$$

The gain of the velocity and the acceleration errors is given by (19)

$$\frac{v_{ri}}{v_{ri-1}} = \frac{a_{ri}}{a_{ri-1}} = \frac{(1 - G_i)}{(1 - G_{i-1})} G_{i-1} = \bar{G}_i(s)$$

where

$$\bar{G}_i = \frac{(1 - G_{th})}{(1 - G_p)} G_p = \frac{0.37s^3 + 0.074s^2 + 0.0037s}{1.5s^5 + 3.1s^4 + 1.775s^3 + 0.268s^2 + 0.012s} = \tilde{G}_{ii-1}(s).$$

Calculating the impulse responses of the above two error systems, we get

$$g_{ii-1}(t) = 0.051e^{-1.12t} - 0.05e^{-0.222t} - 0.016e^{-0.107t} + 0.014e^{-0.094t}$$

and

$$\tilde{g}_{ii-1}(t) = -0.463e^{-1.2t} + 0.463e^{-0.667t}.$$

We find that $\|g_{ii-1}\|_1 = 0.175$ and $\|\tilde{g}_{ii-1}\|_1 = 0.308$ which shows that the semiautomated vehicle (vehicle i in Fig. 6) attenuates the position, velocity and acceleration errors (from the manually driven vehicle $i-1$ in Fig. 6) and does not contribute to the slinky effect phenomenon. On the other hand, if vehicle i were a manually driven vehicle in manual vehicle traffic, the error propagation would be given by $\|g_p\|_1 = 1.1$ as shown in Section III, from which we could not exclude the possibility of error amplification or the existence of slinky-type effects.

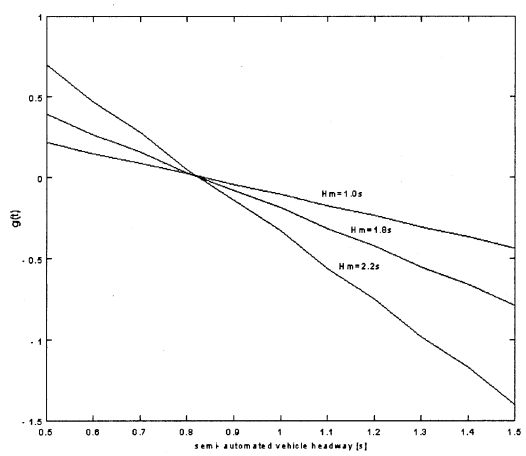

(a)

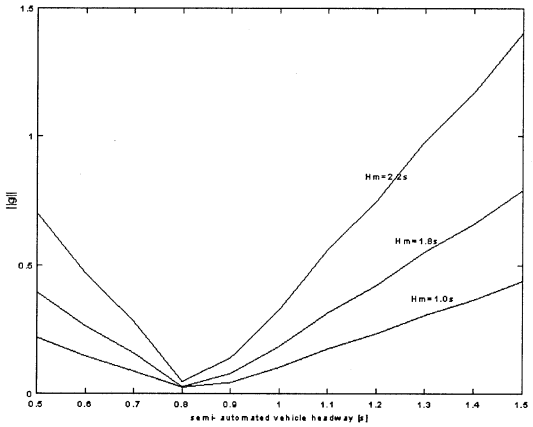

(b)

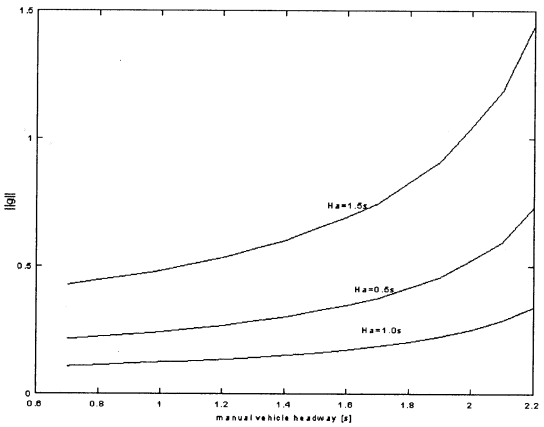

(c)

Fig. 7. (a): Area under the curve of $\|g_{ii-1}\|_1$ as a function of semiautomated vehicle headway from $0.5s$ to $1.5s$ for different manual vehicle headways of $1.0s, 1.8s$, and $2.2s$. (b) $\|g_{ii-1}\|_1$ as a function of semiautomated vehicle headway from $0.5s$ to $1.5s$ for different manual vehicle headways of $1.0s, 1.8s$, and $2.2s$. (c) $\|g_{ii-1}\|_1$ as a function of manual vehicle headway from $0.6s$ to $2.2s$ for different semiautomated vehicle headways of $0.5s, 1.0s$, and $1.5s$.

We can verify from (21) that the impulse response $g_{ii-1}(t)$ of $G_{ii-1}(s)$ depends on the headways of manual and semiautomated vehicles. It is possible to have manual vehicles follow headways other than the mean value of $1.8s$. Also some semiautomated vehicles may be programmed to use headways other than $1.0s$. To carry out the above analysis under such varied sit-

uations, we can use the plots in Fig. 7. The area under the curve of $g_{ii-1}(t)$ is plotted in Fig. 7(a) as a function of the semiautomated vehicle headway from $0.5s$ to $1.5s$ for different manual vehicle headway of $1.0s, 1.8s$, and $2.2s$, and is a linear function of h_i, the semiautomated vehicle headway. The $\|g_{ii-1}\|_1$ is plotted in Fig. 7(b) while Fig. 7(c) plots $\|g_{ii-1}\|_1$ as a function of manual vehicle headway from $0.7s$ to $2.2s$ for different semiautomated vehicle headway of $0.5s$, $1.0s$, and $1.5s$. Using Lemma 3, we can show that for $h = 1/1.2$ we have $\|g_{ii-1}\|_1 = 0$ as seen in Fig. 7(b).

To analyze the effect of error attenuation by a semiautomated vehicle on the following vehicle, let us consider the position, velocity and acceleration errors for manual vehicle $i+1$. We have

$$\begin{aligned}\frac{\delta_{i+1}}{\delta_i} &= \frac{1 - G_p - 1.8sG_p}{1 - G_{th} - sG_{th}} G_{th} \\ &= -\frac{1.8s^4 + 0.7608s^3 + 0.0982s^2 + 0.004s}{0.3s^5 + 0.26s^4 + 0.117s^3 + 0.0168s^2 + 0.0007s} \\ &= G_{ii+1}\end{aligned}$$

and

$$\begin{aligned}\frac{v_{ri+1}}{v_{ri}} = \frac{a_{ri+1}}{a_{ri}} &= \frac{(1 - G_p)}{(1 - G_{th})} G_{th} \\ &= \frac{1.8s^4 + 1.56s^3 + 0.258s^2 + 0.012s}{1.5s^5 + 1.3s^4 + 0.585s^3 + 0.084s^2 + 0.0037s} \\ &= \tilde{G}_{ii+1}.\end{aligned}$$

The impulse responses are given by

$$\begin{aligned}g_{ii+1}(t) = &-5.99e^{-0.333t}\cos(0.369t) \\ &+ 1.829e^{-0.333t}\sin(0.369t) \\ &+ 0.041e^{-0.127t} - 0.051e^{-0.074t} \\ \tilde{g}_{ii+1}(t) = &\, 1.2e^{-0.333t}\cos(0.368t) \\ &+ 1.086e^{-0.333t}\sin(0.368t).\end{aligned}$$

We obtain $\|g_{ii+1}\|_1 = 11.78$ and $\|\hat{g}_{ii+1}\|_1 = 3.88$ which shows that the manual vehicle following the semiautomated vehicle may amplify the position, velocity, and acceleration errors. So no conclusion is possible for the tracking errors of vehicle $i+1$ from the above analysis.

B. Lead Manual Vehicle in Mixed Traffic Performs a Rapid Acceleration Maneuver

Using the ICC model for semiautomated vehicles, a rapid acceleration maneuver by the lead manual vehicle means acceleration at a rate greater than $a_{\max}$. In such circumstances, we later demonstrate that the semiautomated vehicle improves traffic flow characteristics. It filters the response of the rapidly accelerating lead manual vehicle in an effort to maintain smooth driving. This is done at the expense of larger position, velocity, and acceleration errors and sometimes at the expense of falling far behind the vehicle ahead when the intervehicle spacing becomes larger than that stipulated by the constant time headway policy. This smoothing of traffic flow by the semiautomated vehicle is beneficial for the environment, as we shall observe in Section VII.

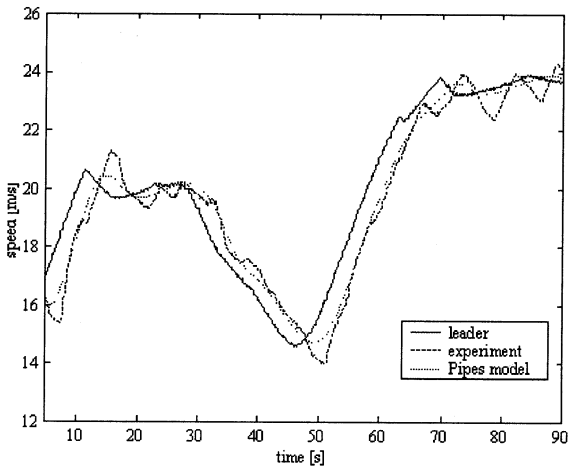

Fig. 8. Comparison of response of Pipes model with an actual manual vehicle response in a manual traffic vehicle following scenario.

VI. Simulations and Experiments

A. Manual Traffic

We compare the Pipes human driver car following model with the response of an actual manual driver. Experiments were conducted using two manually driven vehicles following each other in a single lane. The lead driver was instructed to speed up from 37 mi/h ($\sim$ 17 m/s) to 45 mi/h ($\sim$ 20 m/s), slow down to about 30 mi/h ($\sim$ 14 m/s), and then speed up to 50 mi/h ($\sim$ 23 m/s). The driver of the following vehicle was instructed to follow the lead vehicle using a comfortable time headway. The speed profile generated by the lead vehicle was used as input to the Pipes model in simulation and the response was compared to the response of the actual vehicle. As shown in Fig. 8, the Pipes model gives a smooth approximation of the manual driving response. The experimental vehicle response has greater overshoots and undershoots than the Pipes model. Thus, the results obtained using Pipes model could be viewed as being more conservative than those observed in practice. The experimental comparison results shown in Fig. 8 are found to be similar with several different drivers.

We now simulate different vehicle following scenarios in manual and mixed traffic. Since the objective is to study vehicle following transients, we do not investigate any safety aspects and assume normal vehicle operations with no instances of jeopardizing vehicle safety that might warrant emergency maneuvers.

For our case study, we examine the vehicle following transients in dense manual traffic where a string of 10 manually driven vehicles follow a lead vehicle in a single lane without passing. The lead vehicle accelerates from 0 to 24 m/s with an acceleration of about 0.075 g and the rest of the vehicles follow suit. Fig. 9(a) shows the onset of slinky-type effect in the velocity responses of the following vehicles. We also observe in Fig. 9(b) that the position errors are amplified as they propagate upstream.

B. Mixed Traffic

Let us now consider a string of 10 vehicles following a lead vehicle in a single lane without passing in mixed manual/semiautomated traffic and examine the effect of mixing on the traffic

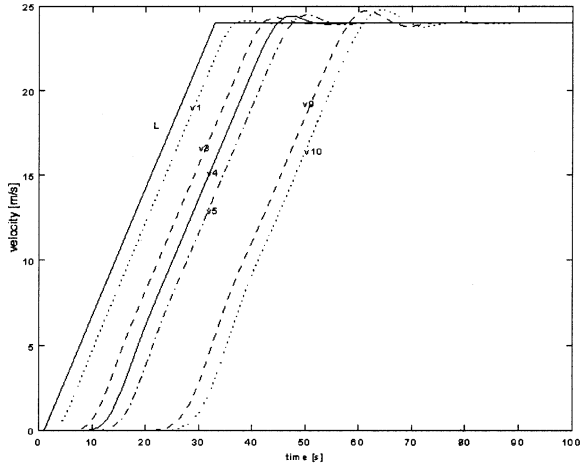

(a)

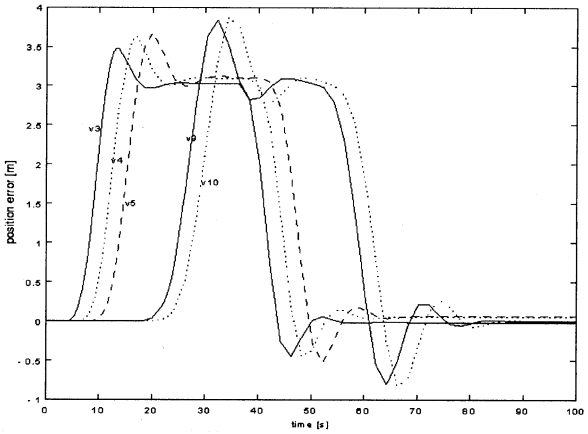

(b)

Fig. 9. Ten vehicles in manual traffic (Pipes model) following a lead vehicle. (a) Velocity response of leader (L), first vehicle (v1), and vehicles 3 to 5 (v3–v5) and 9, 10 (v9, v10). (b) Position error of vehicles 3 to 5 (v3–v5) and 9, 10 (v9, v10).

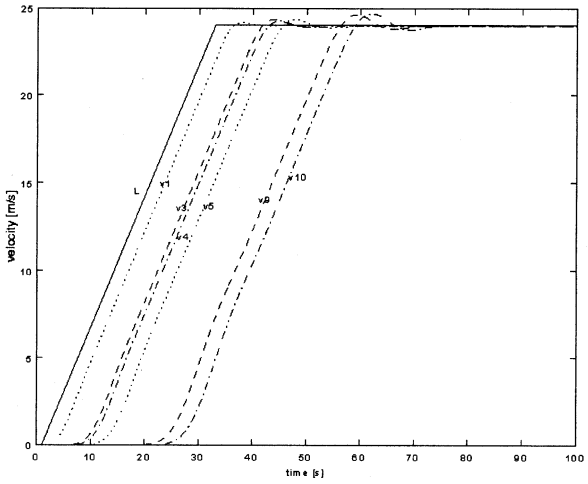

(a)

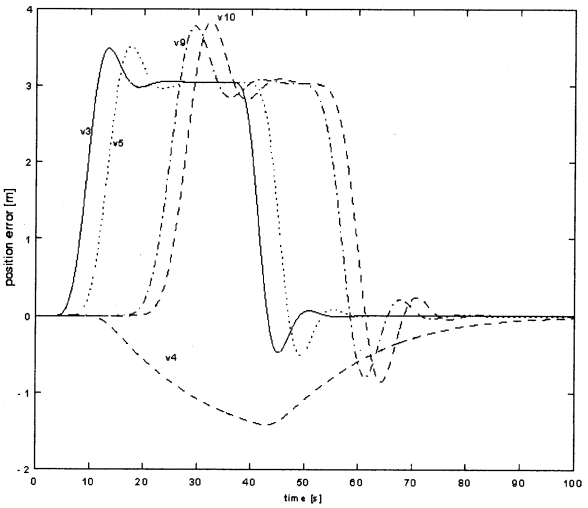

(b)

Fig. 10. Ten vehicles in mixed manual (Pipes model)/semiautomated traffic following a lead vehicle performing smooth acceleration maneuvers. The fourth vehicle (v4) is semiautomated. (a) Velocity response of leader (L), first vehicle (v1), and vehicles 3 to 5 (v3–v5) and 9, 10 (v9, v10). (b) Position error of vehicles 3 to 5 (v3–v5) and 9, 10 (v9, v10).

flow characteristics during transients. The Pipes model which is experimentally shown above to closely model the response of manually driven vehicles is used for simulations. The validated ICC model presented in Section IV is used to simulate semiautomated vehicles. We consider the fourth vehicle to be semiautomated which corresponds to 10% mixing of semiautomated with manual vehicles. We consider two separate cases:

1) smooth acceleration by lead vehicle;
2) rapid acceleration by lead vehicle.

1) Smooth Acceleration by Lead Vehicle: The lead vehicle accelerates smoothly from 0 to 24 m/s at 0.075 g and the rest follow suit. The velocity responses in Fig. 10(a) show good tracking by the semiautomated vehicle v4. It attenuates the position error and does not contribute to the slinky effect phenomenon as shown in Fig. 10(b).

2) Rapid Acceleration by Lead Vehicle: The lead vehicle accelerates at 0.35 g from 0 to 24.5 m/s, maintains a constant speed at 24.5 m/s, thereafter decelerates to 14.5 m/s at 0.3 g and finally accelerates to 24.5 m/s at 0.25 g. The acceleration and deceleration values used are typical for many passenger cars [4]. The simulated braking maneuver is such that it is a safe maneuver and a minimum intervehicle spacing is always maintained for all vehicles. The velocity responses in Fig. 11(a) show that the semiautomated vehicle v4 filters the response of the rapidly accelerating vehicle v3 in an effort to maintain smooth driving. As a result, the responses of vehicles v5, v9, and v10 are less oscillatory than that of v1 and v3. However, this is done at the expense of large position error in v4 [Fig. 11(b)].

VII. Environmental Impact of Mixed Traffic

A. Introduction

In this section, we explore the benefits of semiautomated vehicles in mixed traffic in terms of pollution and fuel consumption. For traffic simulation models at the microscopic level, vehicle parameters such as second-by-second velocity, acceleration, and grade for each individual vehicle determines the emission levels and fuel consumption [13]. For our simulation, we assume that the vehicles travel in a flat road with no change in

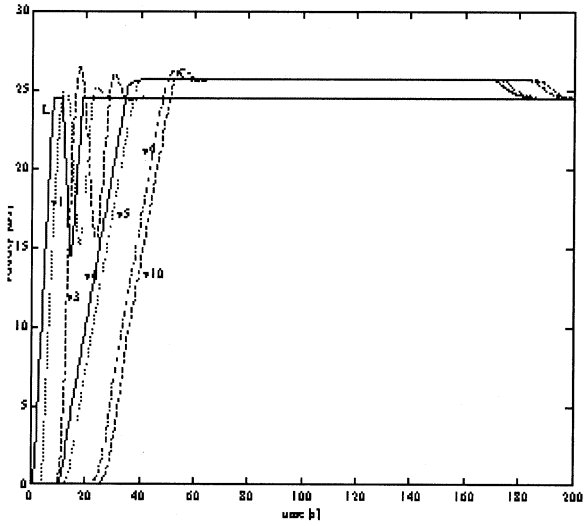

(a)

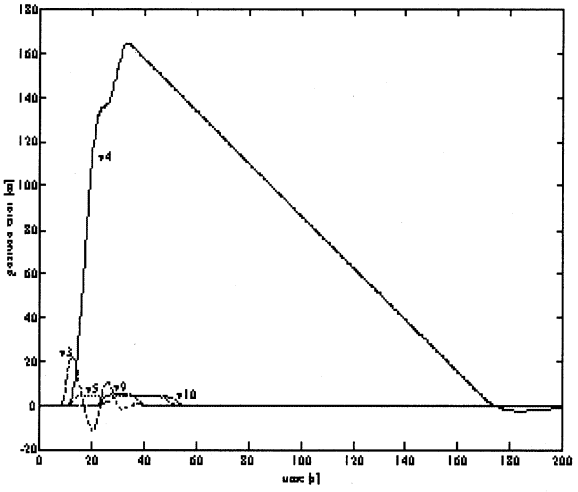

(b)

Fig. 11. Ten vehicles in mixed manual (Pipes model)/semiautomated traffic following a rapidly accelerating lead vehicle. The fourth vehicle (v4) is semiautomated. (a) Velocity response of leader (L), first vehicle (v1), and vehicles 3 to 5 (v3–v5) and 9, 10 (v9, v10). (b) Position error of vehicles 3 to 5 (v3–v5) and 9, 10 (v9, v10).

grade and no wind gusts. Secondary variables such as accessories like air-conditioning are neglected.

The quantities measured are the tailpipe emissions of unburnt hydrocarbons (HC), carbon monoxide (CO), CO_2, oxides of nitrogen (NO, NO_2, denoted by NO_x in this paper), and fuel consumption. The Comprehensive Modal Emissions Model (CMEM) version 1.00 developed at the University of California, Riverside is used to analyze the vehicle data and calculate the air pollution and fuel consumption [14]. It is a high-fidelity, recently developed model that is more sensitive to transients than previous TRAF models [10]. The model calculates vehicle emissions and fuel consumption as a function of the vehicle operating mode, i.e., idle, steady state cruise, various levels of acceleration/deceleration, among others. The inputs to the software are two files: file-ctr and file-act. The first one is the control file that sets vehicle parameters such as units, secondary load, and vehicle category, among others. For our purpose, we use English units and category 5, i.e., high-mileage, high power-to-weight cars, which is the most common vehicle type in California. The second file records the vehicle activity. For our case, it is the recorded vehicle longitudinal speed. The outputs generated by the software are file-sbs and file-sum. The first one records the second-by-second tailpipe emissions of CO, HC, oxides of nitrogen (NO_x), CO_2, and fuel consumption. The second file gives a summary of these values for the trip.

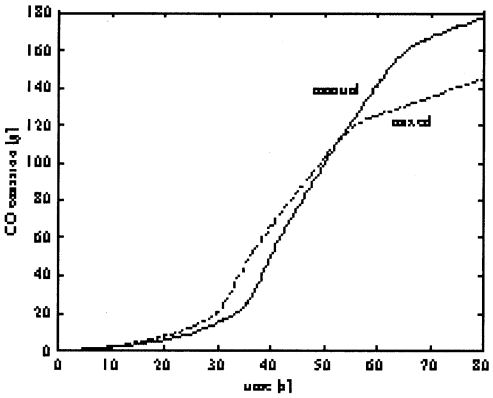

Fig. 12. Comparisons between manual and mixed traffic for smooth acceleration maneuvers for emissions.

TABLE I
PERCENTAGE SAVINGS IN POLLUTION EMISSION AND FUEL CONSUMPTION FOR MIXED TRAFFIC OVER MANUAL TRAFFIC (SIMULATION RESULTS)

	Smooth Acceleration	Rapid Acceleration
CO emission	18.4%	60.6%
CO_2 emission	8.1%	19.8%
NO_x emission	13.1%	1.5%
HC emission	15.5%	55.4%
Fuel consumption	8.5%	28.5%

B. Simulations

We examine the possible environmental benefits due to the presence of semiautomated vehicles in mixed traffic using the simulations in Section VI for a string of 10 vehicles following a lead vehicle in a single lane without passing.

1) Smooth Acceleration: The lead vehicle accelerates smoothly from 0 to 24 m/s at 0.075 g and the rest follow suit. The total CO emissions by manual traffic are compared with that of mixed traffic in Fig. 12. Similar environmental benefits are achieved for HC, CO_2, NO_x emissions and fuel consumption, as tabulated in Table I. Thus, the accurate speed and position tracking of the semiautomated translates into lower air pollution and fuel savings.

2) Rapid Acceleration: When the lead manual vehicle performs rapid acceleration maneuvers as in Fig. 10, the pollution emissions and fuel consumption in manual traffic can be con-

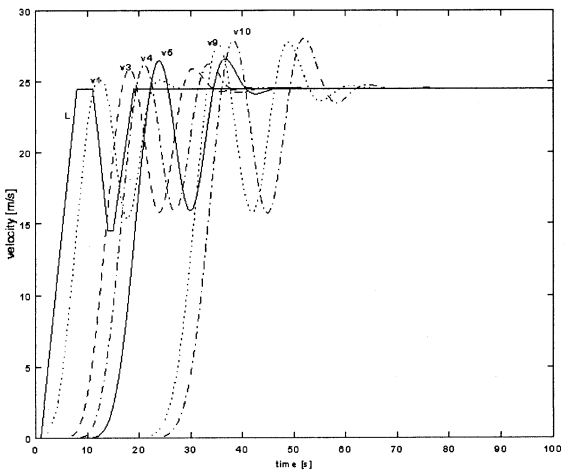

Fig. 13. Ten manually driven vehicles follow a rapidly accelerating leader. Velocity response of leader (L), first vehicle (v1), and vehicles 3 to 5 (v3–v5) and 9, 10 (v9, 10).

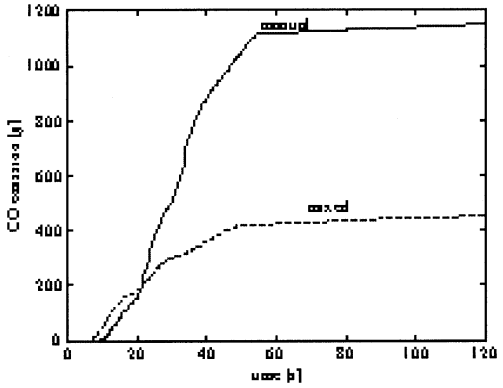

Fig. 14. Comparisons between manual and mixed traffic for rapid acceleration maneuvers for emissions.

siderably reduced due to the presence of the semiautomated vehicle. Fig. 13 shows the velocity responses of six vehicles in a string of 10 manually driven vehicles following a lead vehicle performing rapid acceleration maneuvers as in Fig. 11. The total CO emissions by manual traffic (Fig. 13) are compared with that of mixed traffic (Fig. 11) in Fig. 14. The significant pollution improvement and fuel savings due to smoothing of traffic flow by the semiautomated vehicle are tabulated in Table I.

C. Experiments

The aim is to perform experiments using actual vehicles to investigate the validity of the theoretical results developed in Section VII-B. The experiments would be for two types of traffic—fully manual in which all vehicles are under manual control and mixed in which a single (semiautomated) vehicle is equipped with ICC system while the rest are manually driven. Three vehicles were used for the experiments, with one changing to ICC system for the mixed traffic scenarios.

The ICC software was implemented on a Ford Lincoln experimental vehicle. The ICC controller uses range and range rate measurements from the forward looking ranging sensor. However, due to noise corruption, no range rate data was available. So the algorithm was modified to do a differentiation

TABLE II
PERCENTAGE SAVINGS IN POLLUTION EMISSION AND FUEL CONSUMPTION FOR MIXED TRAFFIC OVER MANUAL TRAFFIC

	Smooth Acceleration		Rapid Acceleration	
	Experiment	Simulation	Experiment	Simulation
CO emission	1.2%	0.8%	19.2%	12.3 %
CO_2 emission	0.4%	0.2%	3.4%	3.3%
NO_x emission	1.6%	1.3%	25.7%	19.2 %
HC emission	0.8%	0.4%	9.8%	6.6%
Fuel consumption	0.4%	0.2%	3.6%	3.4%

of the range, taking the difference between the current range and the previous range over the time interval. This gave us a "pseudo range rate," albeit with a time delay. The variables that were recorded in the Ford Lincoln are: date/time stamp, intervehicle spacing, longitudinal acceleration, desired longitudinal speed, measured longitudinal speed, desired throttle angle, measured throttle angle, desired brake pressure, measured brake pressure, position error, filtered time headway, brake on/off, range rate. The other two vehicles were Buick LeSabre and they were equipped with data acquisition systems to record the speed and intervehicle spacing, i.e., the distance to the lead vehicle if present. Details of the experiments are given in [12].

For manual traffic, all vehicles were operated manually. The driver in the lead vehicle was instructed to follow a smooth speed profile to the best of his/her abilities. The drivers of the following vehicles responded by following the vehicle ahead with a comfortable headway. The vehicles were interchanged for different runs. For mixed traffic experiments, the ICC algorithm was implemented on the Ford Lincoln which was used along with the two Buick LeSabres. A time headway of $1.0s$ was used in the semiautomated vehicle. The lead vehicle performed as closely as possible the same type of maneuvers as in manual traffic. The ICC (Ford) vehicle was placed as the second vehicle for the runs. The manual vehicles position was interchanged for different runs. The speed data collected from the experiments was analyzed using CMEM.

Three vehicles were used in the experiments since it was not possible to use 10 vehicles. Therefore, to see how the simulation results compare with the experimental results, we reran the simulations using only two vehicles following a lead vehicle in manual traffic and mixed traffic. The lead vehicle speed profiles obtained during the experiments were used. The speed responses of the models were collected and analyzed using CMEM. The environmental benefits measured due to the presence of the semiautomated vehicle during experiments and simulations are presented in Table II. The simulation results are conservative compared to environmental benefits in actual driving, a consequence of the fact that the Pipes model gives a smooth approximation of actual manual driving.

VIII. Traffic Flow During the Presence of Rapid Acceleration Transients

In this section, we examine the effect of mixed traffic on the highway capacity and the traffic flow during transients and disturbances. Traffic flow is the number of vehicles passing a stationary observer on a highway measured per unit of time. Highway capacity is the theoretical maximum traffic flow on a highway without violating safety.

Theoretically, the percentage increase of semiautomated vehicles in mixed traffic increases the traffic flow at steady-state conditions due to the smaller time headways used by the ICC vehicles [11]. The question, however, is whether the "sluggish" response of the ICC vehicles that is responsible for the environmental benefits shown in Section VII affects traffic flow in the presence of traffic disturbances. We answer this question by performing the following simulations for manual and mixed traffic. Consider a stretch of road of length 2.5 km subdivided into five sections of 500 m each. A constant traffic flow is assumed along the road. The manual vehicle dynamics are modeled using the Pipes linear car-following model from Section III and the semiautomated vehicle dynamics are modeled using the ICC design presented in Section IV. All vehicles follow a constant time headway policy. The time headways for the manual vehicles are generated according to a lognormal distribution given in [19] while for semiautomated vehicles they are taken as $1.0s$. It is important to note that the time headway defined in [19] is the time taken to cover the distance that includes the vehicle length. The maximum value for the manual vehicle time headway is taken as $2.5s$. This is done to make the study applicable to current manual traffic where seldom a vehicle in moderately dense traffic conditions uses a time headway greater than $2.5s$. To calculate the traffic flow rate, we count the number of vehicles crossing a point of the highway. Assuming a detector at the end of Section V on the road, we count the number of vehicles that cross the end of Section V over a specified time interval and then average that to get the flow rate in vehicles per hour per lane (veh/h/lane). The specified measurement interval for traffic flow is taken to be 60 s. The simulation is run for 600 s that gives 10 measurements of traffic flow. We first consider manual traffic and then mixed traffic with 10% semiautomated vehicles. The semiautomated vehicles are placed randomly among the manually driven ones.

Initially, all vehicles are traveling at 15 m/s. Then after 60 s, when the first traffic flow count has been measured, the lead vehicle in Section V accelerates away rapidly at 0.3 g and the rest of the vehicles follow suit. In mixed traffic, if the lead vehicle in Section V is a semiautomated vehicle, then it accelerates at its maximum value of 0.1 g.

In Fig. 15(a) and (b), we plot the time headways of the vehicles on the highway at the start of the simulation in manual and mixed traffic, respectively. As seen, there are numerous manual vehicles with time headway $2.5s$, since that is the stipulated upper limit. Also in Fig. 15(b) the semiautomated vehicles can be seen with time headway of $1.0s$. Fig. 16 shows the traffic flow for the manual and mixed traffic. There is no significant effect of the rapid acceleration transients on the mixed traffic flow. This is so because transient phenomena do not affect the steady-state traffic flow. The effect of the large intervehicle spacing (and position error) of semiautomated vehicles is absorbed when aggregated over time. Furthermore, the average mixed traffic flow is greater than the manual traffic flow, as expected. Moreover, Fig. 17 shows the average traffic speed for each section. It increases from 15 m/s after 60 s when the lead vehicle in Section V begins to rapidly accelerate. Also, some speed increase can be seen propagating over to Section IV of the road.

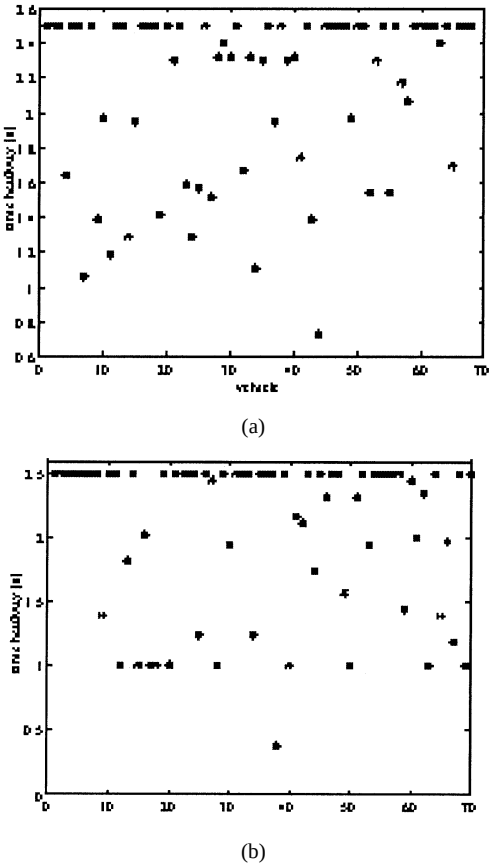

Fig. 15. Time headway of vehicles at initial condition on a 2500-m highway stretch during (a) manual and (b) mixed traffic.

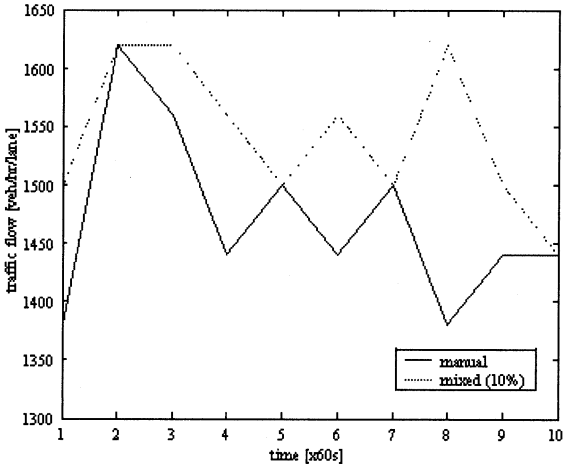

Fig. 16. Traffic flow measured aggregated over 60-s time intervals for manual and mixed traffic when the lead vehicle on the highway rapidly accelerates.

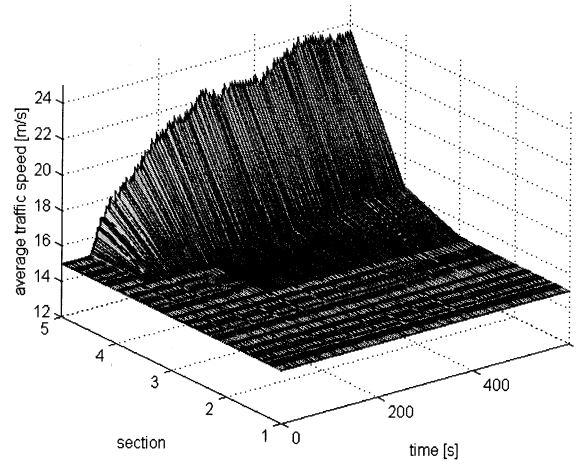

(a)

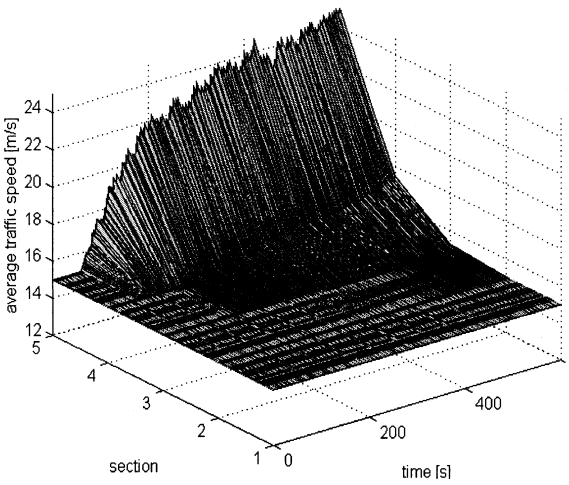

(b)

Fig. 17. Average traffic speed in five sections in (a) manual and (b) mixed traffic when the lead vehicle in section 5 rapidly accelerates.

IX. Conclusion

In this paper we analyzed and simulated mixed manual/semi-automated traffic. The findings suggest the following.

- Semiautomated vehicles in mixed traffic do not contribute to the slinky-effect phenomena during smooth transients.
- Semiautomated vehicles in mixed traffic smooth traffic flow by filtering the response of rapidly accelerating lead vehicles.
- The presence of semiautomated vehicles in mixed traffic improves air pollution levels and fuel savings during transients without adverse effects on the traffic flow rate.

References

[1] P. Ioannou and T. Xu, "Throttle and brake control," *IVHS J.*, vol. 1, no. 4, pp. 345–377, 1994.
[2] P. Ioannou and A. Bose, "Evaluation of mixed automated/manual traffic," report, USC CATT Rep. 97-09-10, Sept. 1997.
[3] A. Bose and P. Ioannou, "Issues and analysis of mixed semi-automated/manual traffic," SAE Tech. Paper Ser. 981943, 1998.
[4] *Consumers Reports Online*, 1998.
[5] M. J. Barth, "The effect of AHS on the environment," in *Automated Highway Systems*, P. Ioannou, Ed. New York: Plenum, 1997.
[6] S. Sheikholeslam and C. A. Desoer, "Longitudinal control of a platoon of vehicles with no communication of lead vehicle information," in *Proc. 1991 American Control Conf.*, Boston, MA, pp. 3102–3106.
[7] C. A. Desoer and M. Vidyasagar, *Feedback Systems: Input–Output Properties*. New York: Academic, 1975.
[8] L. A. Pipes, "An operational analysis of traffic dynamics," *J. Appl. Phys.*, vol. 24, pp. 271–281, 1953.
[9] P. E. Chandler, R. Herman, and E. W. Montroll, "Traffic dynamics: Studies in car following," *Oper. Res.*, vol. 6, pp. 165–184, 1958.
[10] FHWA TRAF Simulation Model Emissions Maps.
[11] P. Ioannou and A. Bose, *Automated Vehicle Control, Handbook of Transportation Science*, R. Hall, Ed. Norwell, MA: Kluwer Academic, 1999, pp. 187–232.
[12] A. Bose and P. Ioannou, "Mixed manual/intelligent cruise control (ICC) traffic experiments," USC, Draft Rep., 2000.
[13] M. J. Barth, "Integrating a modal emissions model into various transportation modeling frameworks," presented at the ASCE Conf., San Francisco, CA, Aug. 10–15, 1997.
[14] ——, *CMEM User's Manual*. Riverside: Univ. Calif., 1998.
[15] R. J. Walker and C. J. Harris, "A multi-sensor fusion system for a laboratory based autonomous vehicle," in *Intelligent Autonomous Vehicles IFAC Workshop*, Southampton, U.K., 1993, pp. 105–110.
[16] "Highway Capacity Manual 1985," TRB, National Research Council, Washington D.C., Special Report 209, 1985.
[17] D. Swaroop and J. K. Hendrick, "String stability of interconnected systems," *IEEE Trans. Automat. Contr.*, vol. 41, pp. 349–357, Mar. 1996.
[18] H. Raza and P. Ioannou, "Macroscopic modeling of automated highway systems," in *Proc. 36th IEEE Conf. Decision and Control*, San Diego, CA, Dec. 10–12, 1997, pp. 4764–4770.
[19] S. Cohen, *Concise Encyclopedia of Traffic and Transportation Systems*, M. Papageorgiou, Ed. New York: Pergamon, 1991, pp. 139–143.

Arnab Bose (S'96–M'01) received the B.Tech. degree in electrical engineering fromthe Indian Institute of Technology, Kharagpur, in 1996 and the M.S. and Ph.D. degrees in electrical engineering from the University of Southern California, Los Angeles, in 1998 and 2000, respectively.

He is currently a Senior Research Engineer with Real-Time Innovations, Inc., Sunnyvale, CA. His research interests are in the areas of embedded and real-time control systems, vehicle dynamics and control, intelligent transportation systems, distributed systems, and hybrid systems. Prior to joining RTI, he did research work in design and development of control systems for automated vehicles. He has also worked on modeling and analysis of control of large complex distributed systems and hybrid systems. At RTI, he is currently working on an effort to automate material handling applications. This includes automation of a material handling crane using a real-time controller and reusable software/hardware components. Previously, at RTI he worked on distributed systems modeling, control and simulations technologies. He has authored 2 book chapters and over 10 research papers.

Dr. Bose was awarded the Best Presentation Award at the 1999 American Control Conference and was a recipient of the Dean's Doctoral Merit Fellowship, School of Engineering, University of Southern California.

Petros A. Ioannou (S'80–M'83–SM'89–F'94) received the B.Sc. degree with First Class Honors from University College, London, U.K., in 1978 and the M.S. and Ph.D. degrees from the University of Illinois at Urbana-Champaign, Urbana, in 1980 and 1982, respectively.

In 1982, he joined the Department of Electrical Engineering–Systems, University of Southern California, Los Angeles. He is currently a Professor in the same Department and the Director of the Center of Advanced Transportation Technologies. His research interests are in the areas of adaptive control, neural networks, nonlinear systems, vehicle dynamics and control, intelligent transportation systems, and marine transportation. He was visiting Professor at the University of Newcastle, Australia ,and the Australian National University in Canberra during parts of fall of 1988, the Technical University of Crete in summer 1992 and fall 2001, and served as the Dean of the School of Pure and Applied Science at the University of Cyprus in 1995. He the author/coauthor of five books and over 150 research papers in the area of controls, neural networks, nonlinear dynamical systems, and intelligent transportation systems.

Dr. Ioannou was a recipient of the Outstanding Transactions Paper Award in 1984 for his paper, "An Asymptotic Error Analysis of Identifiers and Adaptive Observers in the Presence of Parasitics," which appeared in the IEEE TRANSACTIONS ON AUTOMATIC CONTROL in August 1982. He is also the recipient of a 1985 Presidential Young Investigator Award for his research in Adaptive Control. He has been an Associate Editor for the IEEE TRANSACTIONS ON AUTOMATIC CONTROL, the *International Journal of Control*, and *Automatica*. He is currently an Associate Editor of the IEEE TRANSACTIONS ON INTELLIGENT TRANSPORTATION SYSTEMS, Associate Editor at Large of the IEEE TRANSACTIONS ON AUTOMATIC CONTROL, Member of the Control System Society on IEEE ITS Council Committee and Vice-Chairman of the IFAC Technical Committee on Transportation Systems.